# Evaluation of both composition and strain distributions in InGaN epitaxial film using x-ray diffraction techniques*

Guo Xi(郭 希)†, Wang Hui(王 辉), Jiang De-Sheng(江德生), Wang Yu-Tian(王玉田), Zhao De-Gang(赵德刚), Zhu Jian-Jun(朱建军), Liu Zong-Shun(刘宗顺), Zhang Shu-Ming(张书明), and Yang Hui(杨 辉)

*State Key Laboratory on Integrated Optoelectronics, Institute of Semiconductors, Chinese Academy of Sciences, Beijing* 100083*, China*

(Received 23 February 2010; revised manuscript received 17 May 2010)

The composition and stain distributions in the InGaN epitaxial films are jointly measured by employing various x-ray diffraction (XRD) techniques, including out-of-plane XRD at special planes, in-plane grazing incidence XRD, and reciprocal space mapping (RSM). It is confirmed that the measurement of (204) reflection allows a rapid access to estimate the composition without considering the influence of biaxial strain. The two-dimensional RSM checks composition and degree of strain relaxation jointly, revealing an inhomogeneous strain distribution profile along the growth direction. As the film thickness increases from 100 nm to 450 nm, the strain status of InGaN films gradually transfers from almost fully strained to fully relaxed state and then more In atoms incorporate into the film, while the near-interface region of InGaN films remains pseudomorphic to GaN.

**Keywords:** InGaN, In-plane grazing incidence x-ray diffraction, reciprocal space mapping, biaxial strain

**PACC:** 6855, 7870C, 7280E, 6110M

## 1. Introduction

InGaN ternary alloys have attracted increasing research interest due to the promising applications in commercial light emitting diodes and laser diodes from blue-violet to green wavelength.[1] Recent studies[2] have shown tremendous potential of InGaN alloys in fabricating high efficiency multi-junction solar cell operating in the whole solar spectrum because the tunable direct band gap of InGaN ranges from infrared region (0.7 eV) to near UV region (3.4 eV).[3] Despite the rapid research developments in the growth of InGaN, realization of InGaN epilayers with high crystalline quality using metalorganic chemical vapour deposition (MOCVD) still remains a very challenging process. Due to the low solubility of InN in GaN and the large solid phase miscibility gap,[4] phase separation and compositional inhomogeneity are commonly observed in InGaN alloys, which may have both advantageous and detrimental effects upon the performances of the devices.[5] On the other hand, large lattice mismatch up to ∼11% between GaN and InN gives rise to considerable misfit strain present in the InGaN heteroepitaxial films on GaN. Plastic relaxation of misfit strain occurs when film thickness exceeds the critical thickness and results in defect generation such as misfit dislocations and V-pits.[6] Experimental observations of splitting double x-ray diffraction peaks and luminescence lines in InGaN alloys are used to be considered as the evidence of compositional inhomogeneity.[7] Also the phenomenon is correlated to the strain relaxation during the growth process.[8] The precise knowledge of composition and strain plays an important role in the design and fabrication of InGaN-based optoelectronic devices.[9,10] As a result, it is necessary to make a thorough study on

*Project supported by the National Natural Science Foundation of China (Grant Nos. 60506001, 60776047, 60976045, and 60836003), the National Basic Research Programme of China (Grant No. 2007CB936700) and the National Natural Science Foundation for Distinguished Young Scholars (Grant No. 60925017).

†Corresponding author. E-mail: guox@semi.ac.cn

© 2010 Chinese Physical Society and IOP Publishing Ltd

the chemical composition taking the strain relaxation into consideration.

The x-ray diffraction (XRD) is now well established as a powerful and nondestructive tool for structural characterization.[11] It is especially suitable for making strain and lattice parameter evaluation in comparison with other methods due to its high sensitivity to lattice plane displacements. The chemical composition of InGaN films has commonly been estimated from peak position of XRD (00$l$) reflection in $\omega$–$2\theta$ mode by applying Vegard's law. However, to accurately determine the In content, the influences of strain and composition must be separated and analysed quantitatively. In this article, we report a detailed XRD study on InGaN films grown on GaN templates with varying thickness. A variety of methods are carried out to assess the composition and strain distributions using out-of-plane high resolution XRD, in-plane grazing incidence diffraction and reciprocal space mapping (RSM) measurements. The results demonstrate the effects of interplay between composition and strain in InGaN films during growth.

## 2. Experimental procedures

$In_xGa_{1-x}N$ epitaxial films investigated in this study were grown by a conventional horizontal MOCVD reactor equipped with an *in-situ* optical monitor. The precursors were trimethylgallium, trimethylindium and ammonia for Ga, In, and N, respectively. The 2-$\mu$m-thick GaN templates were grown on (001) sapphire substrates at 1040 °C prior to the growth of InGaN films. Three different samples A, B, C with typical thicknesses of 100, 200 and 450 nm were deposited under nearly the same growth conditions, at 700 °C and a growth rate of 0.18 $\mu$m/h. The thicknesses of the films were obtained from *in-situ* optical interference measurement during the growth.

The x-ray measurements were performed on a Bruker D8 DISCOVER high-resolution x-ray diffractometer equipped with a Cu sealed-tube and a four-circle goniometer. The highly monochromatic and quasi-parallel CuK $\alpha$1 x-ray beam ($\lambda$ = 1.54056 Å, 1 Å = 0.1 nm) were produced using a four-bounce asymmetric Ge(220) monochromator. In order to enhance the collected x-ray intensities, a 100-$\mu$m wide receiving slit was put in front of the x-ray detector instead of the crystal analyser. The InGaN/GaN heterostructures were examined with a series of $\omega$–$2\theta$ scans about (004) and (204) reflections. The asymmetric RSMs around (105) Bragg peaks of InGaN and GaN layers were also carried out. To measure the (100) reflection in the in-plane grazing incidence geometry, x-ray tube was rotated 90° and the samples were placed in a horizontal direction so that the scattering plane was almost parallel to the sample surface. A parabolic multilayer mirror (Göbel mirror) and double Soller Slit were employed to obtain high intensity and low divergence angle of the incoming beam.

## 3. Results and discussion

Figure 1(a) shows the $\omega$–$2\theta$ (004) reflection of InGaN film samples A, B, and C grown on GaN/$Al_2O_3$ templates. The dominant peaks marked as "GaN" are the characteristic peaks of thick GaN templates, and the peaks at lower angles correspond to InGaN epitaxial films. There are no multiple InGaN peaks in the XRD pattern of sample A, implying a compositionally uniform film. Figures 1(b) and 1(c) show the detailed $\omega$–$2\theta$ (004) reflection of samples B and C around InGaN peaks. As shown in illustration, these curves are asymmetric, and two-component InGaN peaks are revealed by fitting. The pseudo-Voigt line shape, which is a convolution of a Gaussian and a Lorentzian function, is used to fit the data. The results show that the peak position of weaker shoulders for samples B and C is consistent with the InGaN peak position of sample A, which implies that these peaks can be attributed to the similar InGaN initial portion growing close to GaN templates, and in Figs. 1(b) and 1(c) the stronger peaks of samples B and C are attributed to the top part of InGaN layers (as proved by the RSMs below). The significant shift and broadening of InGaN reflection peaks demonstrate an inhomogeneous distribution of strain and composition which requires further analysis.

Lattice parameter determination provides information on both composition and residual strain of the films. On the basis of Bragg law, $n\lambda = 2d_{hkl}\sin\theta$, the Bragg angle $\theta$ is used to acquire the spacing $d_{hkl}$ between a particular set of planes. Taking the GaN (004) peak as a reference, the lattice parameter $c$ of InGaN can be precisely determined by finding the angular separation of the layer peak from the reference GaN peak, given the relative mismatch between them,

as shown in Fig. 1. Assuming the epitaxial film to be fully relaxed, the lattice parameter is only affected by the chemical composition. Therefore, according to the Vegard's law, which states that a ternary alloy shows a linear dependence of lattice parameter on composition, the In composition can be derived from the plane spacing measured in one specific direction. Under the above-mentioned assumption, the In composition $x$ is extracted from the out-of-plane lattice parameter $c$ or in-plane lattice parameter $a$ of alloy film, by the following expressions:

$$c(x) = c_0^{\mathrm{GaN}}(1-x) + c_0^{\mathrm{InN}}x,$$
$$a(x) = a_0^{\mathrm{GaN}}(1-x) + a_0^{\mathrm{InN}}x, \quad (1)$$

where the fully relaxed lattice parameter for GaN and InN are $c_0^{\mathrm{GaN}} = 5.1850$ Å, $a_0^{\mathrm{GaN}} = 3.1892$ Å, $c_0^{\mathrm{InN}} = 5.7033$ Å and $a_0^{\mathrm{InN}} = 3.5378$ Å, respectively.[12,13]

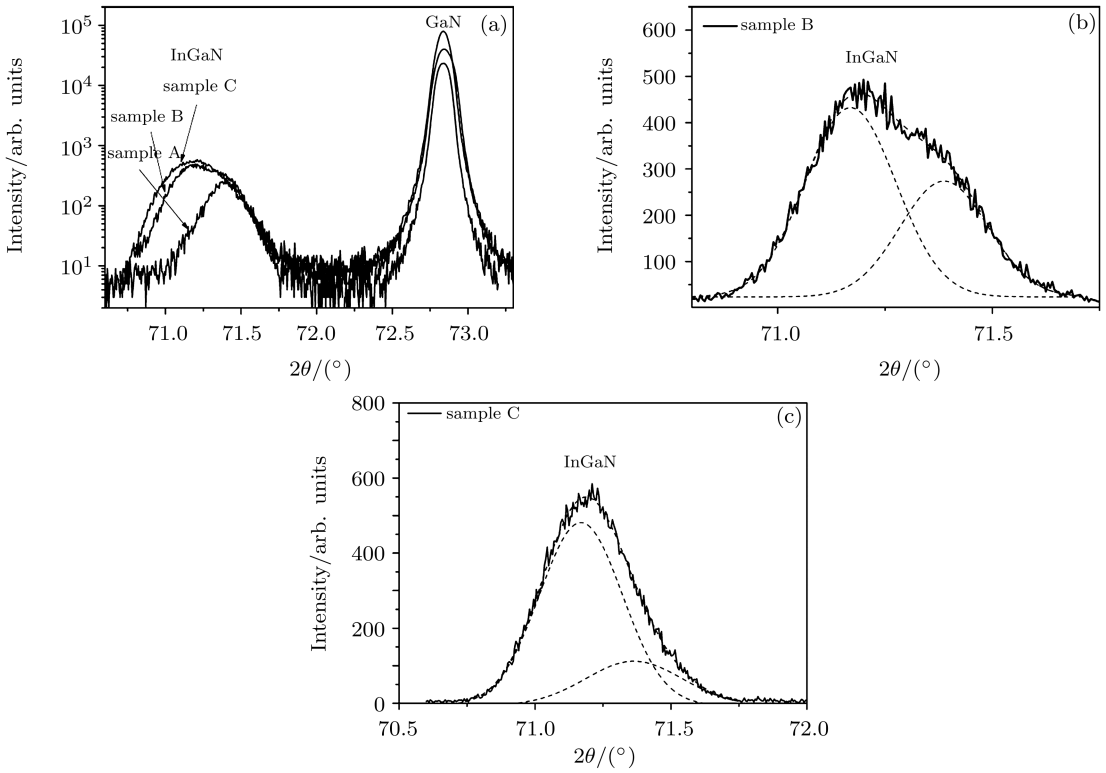



**Fig. 1.** (a) Triple-axis $\omega$–$2\theta$ scans of the (004) reflection from InGaN/GaN heterostructures of samples A, B, and C. (b) Detailed InGaN $\omega$–$2\theta$ (004) reflection and fitting curves of sample B. (c) Detailed InGaN $\omega$–$2\theta$ (004) reflection and fitting curves of sample C.

However, in a large mismatched epitaxial system, significant misfit strains are normally present in the epilayers. For strained wurtzite InGaN heterostructure, the strain components $\varepsilon_{xx}$ and $\varepsilon_{zz}$ parallel and perpendicular to the film surface are defined as $\varepsilon_{xx} = [a - a_0(x)]/a_0(x)$ and $\varepsilon_{zz} = [c - c_0(x)]/c_0(x)$, where $a$ and $c$ are measured lattice parameters, while $a_0$ and $c_0$ are the fully relaxed lattice parameters. Based on the biaxial elastic model, the in-plane strain $\varepsilon_{xx}$ shows a linear relationship with the out-of-plane strain $\varepsilon_{zz}$ by the distortion factor $D$ with a negative sign, as expressed by the following formula:

$$D = \frac{\varepsilon_{zz}}{\varepsilon_{xx}} = -\frac{2\nu}{1-\nu} = -\frac{2c_{13}}{c_{33}}, \quad (2)$$

where $\nu$ is the Poisson's ratio and $c_{13}$ and $c_{33}$ are the components of the elastic stiffness tensor. The presence of biaxial strain will lead to a tetragonal distortion of the unit cell. Therefore, both composition and strain induce variations in the spatial distribution of lattice planes. To evaluate and separate the effects caused by these two factors, multiple symmetric or asymmetric reflections must be measured and the shape of the unit cell should be determined to give both strain state and composition of the InGaN

films.

Normally, to determine the in-plane lattice parameter $a$, asymmetric reflections of lattice planes inclined with large angles to the basal plane are performed, and then the lattice parameter $a$ is calculated taking the lattice parameter $c$ into account. Alternatively, in-plane grazing incidence x-ray diffraction can provide a more convenient approach to directly determine the lattice parameter $a$ by measuring the reflection of crystal planes normal to film surface. Furthermore, the separation of the fully strained state and fully relaxed state in the films are more explicitly exhibited in the in-plane grazing incidence diffraction geometry. In our experiments, the grazing incidence angle is set to 0.4°, and corresponding penetration depth is about 80 nm. As depicted in Fig. 2, in the in-plane $\omega$–$2\theta$ (100) reflection of sample A, only one prominent InGaN peak is observed, of which the position is identical to the (100) diffraction angle of reference GaN. It is concluded that the thickness of the InGaN film of sample A is below the critical thickness, therefore the InGaN film is pseudomorphically strained, in which the in-plane lattice parameter of the InGaN matches to the GaN template beneath. It appears that the critical thickness is much larger than the values calculated from the Mathews and Blakeslee (M-B) model and the Fischer model. A similar result was also reported based on photoluminescence and transmission electron microscopy (TEM) measurements.[14,15] When the film thickness exceeds critical thickness, a relaxation of misfit strain is expected to occur through the generation of misfit dislocations. Accordingly, there are two additional diffraction components present in the InGaN (100) reflection of samples B and C in Fig. 2. They originate from the relaxed region which is located close to the surface and above the pseudomorphic region near the interface. Using the same method stated above, the in-plane lattice parameter $a$ can be determined from the angular positions of grazing incidence diffraction in Fig. 2. Combining the measured in-plane and out-of-plane lattice parameters $a$ and $c$, the indium composition is determined using the relationship concerning the tetragonal distortion in biaxially strained crystal[16]

$$x = -\frac{ac(1+\nu) - ac_0^{\mathrm{GaN}} - ac_0^{\mathrm{GaN}}c\nu}{ac_0^{\mathrm{GaN}} - ac_0^{\mathrm{InN}} - ac_0^{\mathrm{InN}}c\nu + ac_0^{\mathrm{GaN}}c\nu}. \quad (3)$$

A variety of the Poisson's ratio values have been reported in the literature, which leads to some differences in the calculated composition $x$. In this work, $\nu = 0.23$ suggested for GaN[17] is used for the calculation, and then the In composition $x$ is deduced as illustrated by solid upward triangles (marked as "$a + c$") in Fig. 4. The method of "$a + c$" involves combining the lattice parameters $a$ and $c$ in two mutually perpendicular directions. However, there is a more convenient approach which can be employed for the direct composition measurements and will be discussed in the following.

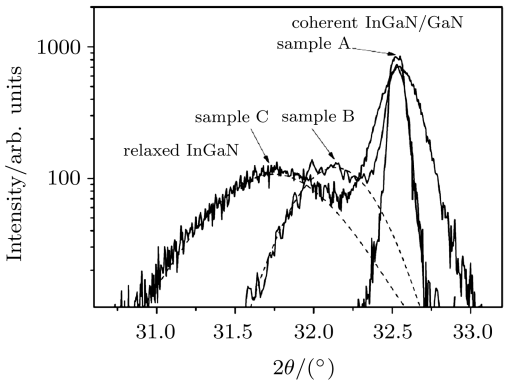



**Fig. 2.** Reflection peaks of samples A, B, and C from the InGaN/GaN (100) planes in in-plane grazing incidence geometry.

It is noticed that the peaks of relaxed InGaN in in-plane (100) reflection of samples B and C shift to lower angles pronouncedly in Fig. 2. The shift increases with increasing film thickness, while in out-of-plane (004) reflection patterns shown in Fig. 1 the corresponding peak displacement of these samples is rather small. The phenomenon is ascribed to the anisotropic property of elastic strain under biaxial stress. In fact, a change in composition will result in the changes of lattice plane spacings in all three dimensions, acting like a hydrostatic pressure. In contrast, for a biaxial strain in the basal plane, the introduced change of the strain component in the perpendicular growth direction is opposite to that of the in-plane component. Therefore, there exists a crystal direction which, during the transformation, turns the stress from compressive (in-plane) to tensile (out-of-plane), so in this direction the atomic spacing is insensitive to the biaxial strain. Thus, we can directly determine the alloy composition in the strained films by measuring plane spacing in such a direction. For wurtzite III-nitrides, this direction is around the normal to the (102) planes with an interplanar angle of 43.2° to (001) plane.[18] Here, the high index skew symmetric (204) reflection is preformed in preference to the (102) reflection to give a greater separation of the peaks. As shown in Fig. 3, two splitting InGaN diffraction components are observed in the $\omega$–$2\theta$ (204) reflection of InGaN films grown on GaN templates in samples B and C, which originate from the relaxed and pseudomorphic InGaN regions, respectively. Therefore, the In compositions

of relaxed InGaN regions in samples B and C can be estimated from peak positions of (204) reflection in $\omega$–$2\theta$ scan mode directly by applying Vegard's law, as shown in Fig. 4 by solid downward triangles (marked as $d_{204}$). The (204) reflection pattern of sample A with the minimum thickness is not presented due to the weak diffraction intensities and size-effect broadening. However, based on the above discussion, we have been able to obtain the In composition in sample A from the reflection peak of the coherent InGaN region which gives the same composition as in sample B or C.

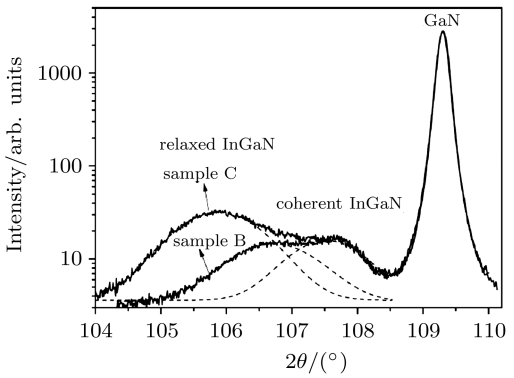



**Fig. 3.** The $\omega$–$2\theta$ scans through the InGaN/GaN (204) reflection peaks of samples B and C.

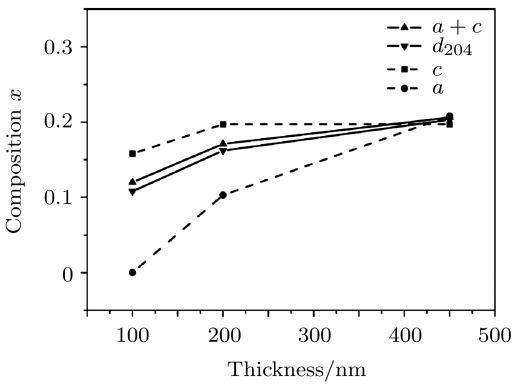



**Fig. 4.** Plot of indium composition $x$ of InGaN films in samples A, B and C as a function of film thickness. The results derived from various methods (see text) are compared.

In Fig. 4, the compositions of the pseudomorphic film in sample A and the relaxed part in samples B and C are plotted versus the layer thickness, where the data estimated from lattice parameter $a$ (solid circles) or parameter $c$ (solid squares) independently, as expected for a fully relaxed layer, are also shown as a reference. It can be seen that the results from (204) reflection are in accordance with the values obtained by the method of combining lattice parameters $a$ and $c$, which confirms the method of (204) reflection can effectively estimate the indium composition from a single measurement. The slight difference between composition values obtained from the two methods is due to the uncertainty of the reference elastic constants. By averaging the values from the two methods, we determine the indium composition in samples A, B, and C to be 0.11, 0.17 and 0.20, respectively.

In order to gain further insight into the composition distribution, strain relaxation process and its correlation with thickness, detailed XRD reciprocal space mapping (RSM) measurements were performed. As compared with diffraction patterns in one-dimensional angular distribution, two-dimensional RSM gives better precision and provides an effective tool for determining the strain states in heterostructures. The degrees of relaxation are defined in the following expression: $R = [a(L) - a_0(s)]/[a_0(L) - a_0(s)]$, where $a(L)$ and $a_0(L)$ are the measured and relaxed in-plane lattice parameter of the InGaN layer, and $a_0(s)$ is the lattice parameter of the GaN template. Both strain and composition gradients will lead to an elongation of broadened reciprocal lattice point (RLP). In asymmetric x-ray reflection, which contains information on both in-plane and out-of-plane plane spacings, the broadenings of the RLP due to composition and strain extend in different directions in the reciprocal space. By assuming that strain state remains unchanged, the elongated line due to composition preserves the relation between $a$ and $c$ in a definite ratio, such as the full ($R = 1$) and zero ($R = 0$) relaxation lines shown as two dashed lines in Fig. 5. The relaxation process from the fully strained state to fully relaxed state of a layer with fixed composition can be illustrated by the isocomposition relaxation line, which inclines at an angle $\alpha$ with respect to the $Q_z$ axis as shown by the solid line in Fig. 5.[19] The angle $\alpha$ can be expressed by the following equation

$$\alpha(x) = \arctan\left(\frac{\tan\varphi}{D(x)}\right), \tag{4}$$

where $\varphi$ is the angle between surface normal and the $(hkl)$ diffraction plane given by the expression

$$\tan\varphi = \frac{c}{a}\sqrt{\frac{4}{3}\frac{(h^2+hk+k^2)}{l^2}}, \tag{5}$$

and $D(x)$ is given by

$$D(x) = 2c_{13}(x)/c_{33}(x). \tag{6}$$

Therefore, we can extract the chemical composition and relaxation degree from the asymmetric RSM separately by distinguishing effects from the two factors. The reference elastic constants used here are $c_{13} = 103$ GPa and $c_{33} = 405$ GPa for GaN, as well as $c_{13} = 92$ GPa and $c_{33} = 224$ GPa for InN.[20]

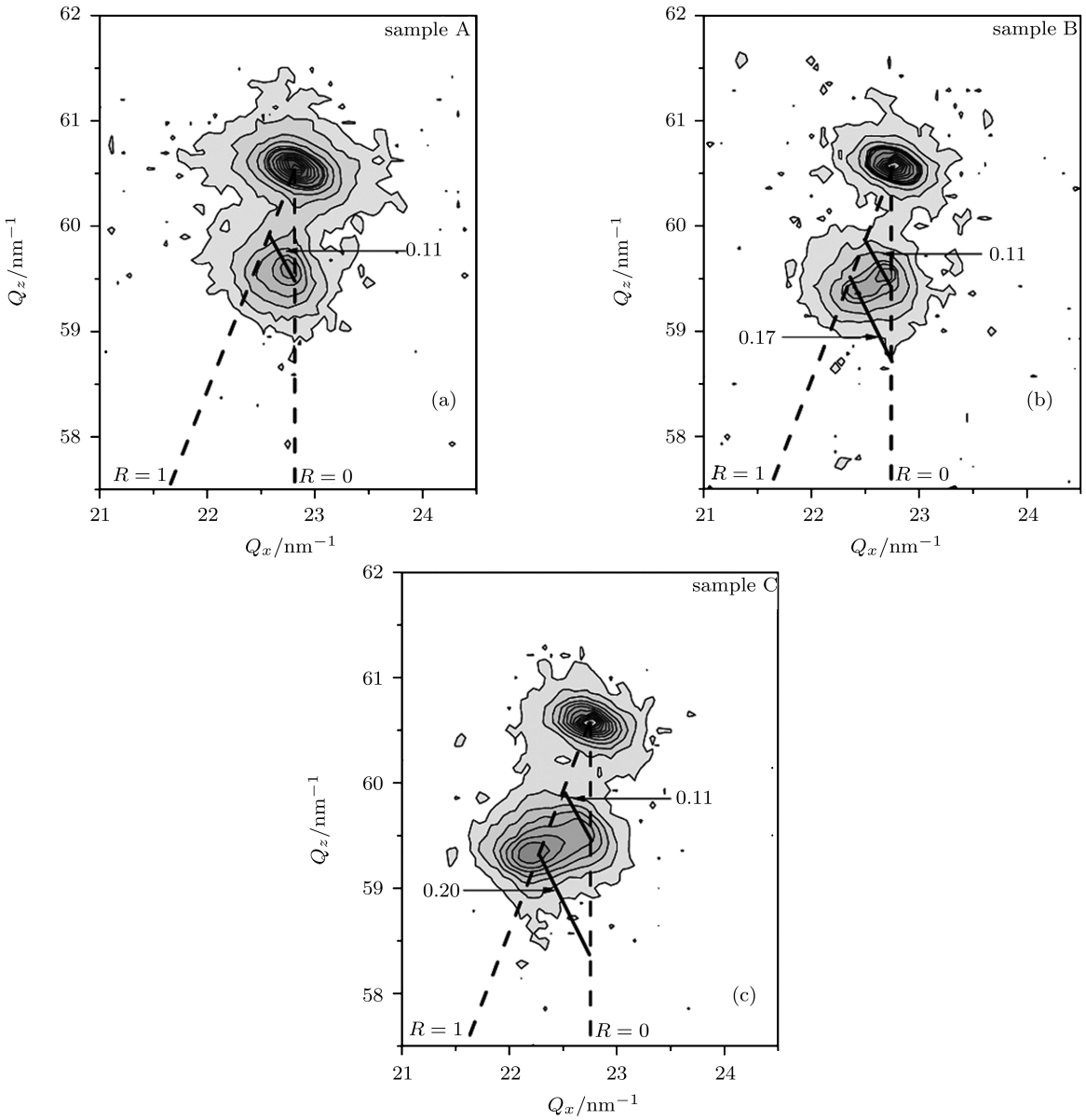



**Fig. 5.** Reciprocal space maps of the (105) reflection from InGaN grown on GaN with varying thickness (samples A, B, and C). The dashed lines passing through the GaN templates RLP correspond to the fully strained ($R = 0$) and fully relaxed ($R = 1$) states. The solid lines between the fully strained and relaxed dashed lines indicate the relaxation directions for different indium compositions noted by arrows.

The asymmetric reciprocal space maps of the (105) diffraction for samples A, B, and C are displayed in Fig. 5. For sample A, the central point with the maximum diffraction intensity of InGaN diffraction profile is nearly located on the vertical line ($R = 0$), close to a fully strained state of the InGaN film. For sample C, which is the most fully relaxed, the maximum of InGaN RLP falls exactly on the full relaxation line ($R = 1$). And the maximum of InGaN RLP in sample B lies between the zero and full relaxation line, indicating a partially relaxed state. By checking the position of InGaN RLP in the isocomposition relaxation line, we can determine the relaxation degree $R$ of sample B to be 0.78. The illustration describes the strain relaxation process in InGaN films as the layer thickness increases and the non-uniform distribution of relaxation degree develops along the growth direction. It can be found that all 3 InGaN layers grow nearly pseudomorphic to GaN at the beginning of the growth, and the relaxed InGaN fraction gradually rises up with increasing relaxation degree during further growth. However, even when the top InGaN layer is fully relaxed, the underlying region very near the interface still remains coherent to the GaN tem-

plate. As the strain states of the films are defined, the compositions can be well extracted from the RSMs as shown in Fig. 5.

The compositions derived from RSMs are in good agreement with the values obtained from analyses presented before by other methods, which further proves the reliability of the analyses using the XRD techniques. An increasing trend of indium composition with increasing thickness of the InGaN films is observed in Figs. 4 and 5, which can be referred to as the so-called compositional pulling effect. When the layer grows pseudomorphic with the underlying GaN template, the strain acts as a factor holding back the indium incorporation in the InGaN lattice, while in the more relaxed region there is a tendency to incorporate higher level of In atoms. Therefore, the correlation effect is well accounted for by the strain distribution in the InGaN films derived from RSM measurements, where a significant relaxation of biaxial strain is confirmed to be present in the growth direction.

## 4. Conclusions

In conclusion, both composition and strain distributions of InGaN epitaxial films with varying thickness grown by MOCVD on GaN templates have been investigated by different means of x-ray diffraction techniques. The spatial distribution of lattice planes in different crystal directions such as out-of-plane lattice parameter $c$, in-plane lattice parameter $a$, and (204) interplanar spacing are directly determined by employing (004) symmetric, (100) in-plane grazing incidence and (204) skew symmetric reflections. There are significant deviations in the estimated In compositions by only considering the lattice parameter $a$ or $c$, demonstrating that the InGaN films are under different amount of biaxial strain. Combining the measured lattice parameters $a$ and $c$, the In composition is determined together with strain. The results are in agreement with compositions extracted from plane spacing measured by XRD in a specific direction of [204] which is insensitive to biaxial strain. The asymmetric (105) RSM is also performed to further investigate the composition and strain distributions in InGaN/GaN heterostructures. The comparative study of different methods gives a useful cross check of the reliability of XRD measurements and minimises the effects of reference elastic constants uncertainties. The results show that the degree of relaxation $R$ is non-uniformly distributed along the growth direction. As the film thickness increases, the biaxial strain in the film progressively relaxes accompanied by an increase of In content toward the surface.

## References


[1] Nakamura S, Senoh N, Iwasa N and Nagahama S I 1995 *Jpn. J. Appl. Phys.* **34** L797

[2] Jani O, Ferguson I, Honsberg C and Kurtz S 2007 *Appl. Phys. Lett.* **91** 132117

[3] Wu J, Walukiewicz W, Yu K M, Ager J W, Haller E E, Lu H and Schaff W J 2002 *Appl. Phys. Lett.* **80** 4741

[4] Singh R, Doppalapudi D, Moustakas T D and Romano L T 1997 *Appl. Phys. Lett.* **70** 1089

[5] Ponce F A, Srinivasan S, Bell A, Geng L, Liu R, Stevens M, Cai J, Omiya H, Marui H and Tanaka S 2003 *Phys. Status Solidi* B **240** 273

[6] Kim I H, Park H S, Park Y J and Kim T 1998 *Appl. Phys. Lett.* **73** 1634

[7] Srinivasan S, Bertram F, Bell A, Ponce F A, Tanaka S, Omiya H and Nakagawa Y 2002 *Appl. Phys. Lett.* **80** 550

[8] Pereira S, Correia M R, Pereira E, Trager-Cowan C, Sweeney F, O'Donnell K P, Alves E, Franco N and Sequeira A D 2002 *Appl. Phys. Lett.* **81** 1207

[9] Tao R C, Yu T J, Jia C Y, Chen Z Z, Qin Z X and Zhang G Y 2009 *Chin. Phys.* B **18** 2603

[10] Yildiz A, Kemal O M, Bosi M, Ozcelik S and Kasap M 2009 *Chin. Phys.* B **18** 4007

[11] Ding Z B, Wang Q, Wang K, Wang H, Chen T X, Zhang G Y and Yao S D 2007 *Acta Phys. Sin.* **56** 2873 (in Chinese)

[12] Detchprohm T, Hiramatsu K, Itoh K and Akasaki I 1992 *Jpn. J. Appl. Phys.* **31** L1454

[13] Paszkowicz W 1999 *Powder Diffr.* **14** 258

[14] Parker C A, Roberts J C, Bedair S M, Reed M J, Liu S X and El-Masry N A 1999 *Appl. Phys. Lett.* **75** 2776

[15] Liu R, Mei J, Srinivasan S, Ponce F A, Omiya H, Narukawa Y and Mukai T 2006 *Appl. Phys. Lett.* **89** 201911

[16] Angerer H, Brunner D, Freudenberg F, Ambacher O, Stutzmann M, Hopler R, Metzger T, Born E, Dollinger G, Bergmaier A, Karsch S and Korner H J 1997 *Appl. Phys. Lett.* **71** 1504

[17] Kisielowski C, Kruger J, Ruvimov S, Suski T, Ager J W, Jones E, Liliental Weber Z, Rubin M, Weber E R, Bremser M D and Davis R F 1996 *Phys. Rev.* B **54** 17745

[18] Wallis D J, Keir A M, Balmer R S, Soley D E J and Martin T 2004 *Appl. Phys. Lett.* **85** 6359

[19] Pereira S, Correia M R, Pereira E, O'Donnell K P, Alves E, Sequeira A D, Franco N, Watson I M and Deatcher C J 2002 *Appl. Phys. Lett.* **80** 3913

[20] Wright A F 1997 *J. Appl. Phys.* **82** 2833